Available online at www.sciencedirect.com
ScienceDirect
International Journal of Pharmaceutics 335 (2007) 46–53
INTERNATIONAL JOURNAL OF PHARMACEUTICS
www.elsevier.com/locate/ijpharm

Examination of penetration routes and distribution of ionic permeants during and after transscleral iontophoresis with magnetic resonance imaging

Sarah A. Molokhia [a], Eun-Kee Jeong [b], William I. Higuchi [a], S. Kevin Li [a,c,*]

[a] *Pharmaceutics and Pharmaceutical Chemistry, University of Utah, Salt Lake City, UT 84112, USA*
[b] *Department of Radiology and Utah Center for Advanced Imaging Research, University of Utah, Salt Lake City, UT 84108, USA*
[c] *Division of Pharmaceutical Sciences, College of Pharmacy, University of Cincinnati, Cincinnati, OH 45267, USA*

Received 23 August 2006; accepted 25 October 2006
Available online 3 November 2006

Abstract

Previously, transscleral and transcorneal iontophoretic delivery was studied and compared to passive delivery and intravitreal injection using nuclear magnetic resonance imaging (MRI). The objective of the present study was to employ MRI to further investigate the factors affecting transscleral iontophoretic delivery. In the present study, anodal and cathodal constant current transscleral iontophoresis were conducted with excised sclera in side-by-side diffusion cells in vitro and with rabbits in vivo. The total current and duration of application were 2 and 4 mA (current density 10 and 20 mA/cm^2) and 20–60 min, respectively. The delivery and distribution of the model permeants manganese ion (Mn^{2+}) and manganese ethylenediaminetetraacetic acid complex ($MnEDTA^{2-}$) into the eye during iontophoresis were determined with MRI and compared with the results obtained in previous studies of subconjunctival injection and passive delivery. Both anodal and cathodal iontophoresis provided significant enhancement in ocular delivery compared to passive transport in the in vitro and in vivo experiments. Transscleral iontophoretic delivery was related to the position and duration of the iontophoresis application in vivo. Permeants were observed to be delivered primarily into the anterior segment of the eye when the pars plana was the application site. Extending the duration of iontophoresis at this site allowed the permeants to be delivered into the vitreous more deeply and to a greater extent than when the application site was at the back of the eye near the fornix. The present results show that electrode placement was an important factor in transscleral iontophoresis, and the ciliary body (pars plana) was determined to be the pathway of least resistance for iontophoretic transport. These new findings continue to support the utility of MRI as a noninvasive technique in ocular drug delivery research and testing.

Keywords: Ocular; Iontophoresis; Transscleral; Drug delivery; MRI

1. Introduction

In recent years, significant progress has been made in optimizing ocular drug delivery. The delivery of therapeutic doses of drugs to the tissues in the posterior segment of the eye, however, remains a significant challenge. Severe vision loss from posterior segment diseases such as age-related macular degeneration, diabetic retinopathy, glaucoma, and retinitis pigmentosa accounts for most cases of irreversible blindness worldwide. Recent interest in drug delivery to the back of the eye has stimulated new interest in ocular iontophoresis. In ocular iontophoresis, a donor electrode containing the drug to be delivered into the eye is placed on the eye. To complete an electrical circuit through the body, another electrode is placed on another body surface. The electric field enhances drug delivery from the donor electrode into the eye. Ocular iontophoresis does not have some of the adverse effects associated with intravitreal or periocular injections and with systemic drug administration. Repeated treatments with injections (intravitreal and periocular) may lead to complications and patient discomfort. Systemic drug administration is often not preferred because of the systemic toxicity involved. In recent studies, ocular iontophoresis has been examined for the treatments of eye diseases (Behar-Cohen et al., 1997; Yoo et al., 2002; Eljarrat-Binstock et al., 2005), and it has been suggested that this technique may allow drug delivery to the back of the eye (Lam et al., 1989; Behar-Cohen et al., 2002; Voigt et

* Corresponding author. Tel.: +1 513 558 0977; fax: +1 513 558 0978.
E-mail address: kevin.li@uc.edu (S.K. Li).

0378-5173/$ – see front matter © 2006 Elsevier B.V. All rights reserved.
doi:10.1016/j.ijpharm.2006.11.001

al., 2002a). Low electric current (density) ocular iontophoresis has also been shown to be relatively safe in animal models and human (Hughes and Maurice, 1984; Behar-Cohen et al., 2002; Voigt et al., 2002a; Parkinson et al., 2003).

Studies employing MRI to follow ocular drug delivery in rabbits have been reported (Li et al., 2004a,b; Kim et al., 2004). An aim of the earlier experiments was to assess MRI as a technique to study ocular delivery and pharmacokinetics in an animal model (Li et al., 2004a,b). In one study, it was found that passive transport of Mn^{2+} and of $MnEDTA^{2-}$ into the eye after subconjunctival injection could not be detected by MRI over a 2-h period after injection in vivo (Li et al., 2004b). However, when the animals were sacrificed before subconjunctival injection in a postmortem experiment, significant penetration of Mn^{2+} and $MnEDTA^{2-}$ into the ciliary body, anterior chamber, and posterior chamber near the injection site was observed after the injection, suggesting the importance of clearance and the blood vasculature barrier in the subconjunctival route. In the second study (Li et al., 2004a), the target sites of ion delivery and the electric current pathways during transscleral and transcorneal iontophoresis were determined and compared using MRI in a rabbit model in vivo. Intravitreal injection and passive delivery were the controls. With short application time, passive diffusion did not deliver a significant amount of the Mn^{2+} into the eye (below detection limit). With 30 min 2-mA anodal constant current, transscleral iontophoresis delivered the ion to the posterior of the eye, and transcorneal iontophoresis delivered the ion into the anterior chamber. However, several questions were not addressed in this previous iontophoresis study. First, the conclusions deduced in the study can be affected by possible specific interactions between the probe ion Mn^{2+} and the eye tissues. There may also be specific ion regulation in the eye altering the pharmacokinetic of the probe ion during and after iontophoresis. Second, the results from an anodal iontophoresis (donor electrode is the anode) study might not hold for cathodal iontophoresis because different electrical polarities could induce different membrane/tissue structural changes. These issues can be studied by using both a cation probe and an anion probe. Third, because of the detection limit of the MRI method, the probe ion at low concentration in the vitreous during and after iontophoresis could not be determined in the previous study. Higher concentration (dose) of the probe ions would be required to provide more complete information of ion distribution in the eye.

The purpose of the present study was to carry out a more systematic study in ocular iontophoresis. More specifically, the following were to be investigated: (1) the efficiency of anodal and cathodal iontophoretic delivery in comparison to subconjunctival injection and passive transport and (2) the interplay of the extent and depth of permeant penetration, electric current, electrode placement, and duration of iontophoresis.

2. Materials and methods

2.1. Materials and animals

$MnCl_2$ tetrahydrate was purchased from Spectrum Chemical (Gardena, CA). Ethylenediamine tetraacetic acid (EDTA) and xylazine were purchased from Sigma Chemical (St. Louis, MO). Ketamine hydrochloride injectable USP (100 mg/ml) was from Hospira Inc. (Lake Forest, IL). Sodium chloride 0.9% USP (pH between 5 and 7) was from Baxter Healthcare (Deerfield, IL). $Na_2MnEDTA$ solutions (with excess EDTA at 1:1.5 Mn:EDTA ratios) were prepared by the chemicals as received and the pH was adjusted to between 5 and 7 by the addition of concentrated NaOH.

For the iontophoresis device, Silastic® flexible tubing (Tygon, 3/16 I.D. × 5/16 O.D.) was purchased from VWR Scientific (San Francisco, CA). Silver foil (1.5 in. × 0.004 in.) was obtained from EM Science (Gibbstown, NJ). Liquid silver paint was from LADD Research Industries (Williston, VT). The iontophoresis devices were constructed as previously described (Li et al., 2004a), with a drug compartment volume of approximately 0.05 ml. Ag was the electrode in the donor chamber in anodal iontophoresis (anode as the donor) and Ag/AgCl was the donor electrode in cathodal iontophoresis (cathode as the donor).

New Zealand white rabbits of 3–4 kg were purchased from Western Oregon Rabbit Co. (Philomath, OR) and were used as the animal model under the approval of the Institutional Animal Care and Use Committee at the University of Utah. In the in vitro experiments, enucleated rabbit eyes were obtained from other studies at the University of Utah Animal Resource Center and harvested from the rabbit carcasses immediately after euthanasia. The sclera tissues were obtained from both the superior and inferior temporal sections after the eye was separated from the rabbits and freed from adhering debris such as the conjunctiva, extraocular muscles, and retina. The area of about 0.4–1 cm from the limbus on the sclera was used.

2.2. In vitro transport experiments

In vitro iontophoresis transport experiments were performed to study the effects of drug concentration upon iontophoretic transport and to demonstrate the principles of the relationships between the permeant physicochemical properties and iontophoretic transport. A two-chamber side-by-side diffusion cell system with excised rabbit sclera was used in the experiments (Li et al., 2004b, 2005). Each compartment of the diffusion cell has a 2-ml volume and an effective diffusional area of around 0.2 cm^2. The sclera was sandwiched between the two half-cells with the choroid side facing the receiver chamber. The diffusion cell was placed in a circulating water bath at $37 \pm 1\,^{\circ}C$. 2 ml saline and 2 ml donor solution were pipetted into the receiver and donor chambers, respectively. The silver foil and Ag/AgCl coated Ag foil were used as the conductive element in anodal and cathodal iontophoresis. Phoresor II Auto constant current iontophoretic device (Model No PM 850, Iomed, Inc., Salt Lake City, UT) was the electric current dose controller for providing the 2 mA electric current. Samples were withdrawn from the donor and receiver chambers at predetermined time (e.g., 20 min) intervals. Typically, 20-μl aliquots were taken from the donor chamber, and 1 ml aliquots were withdrawn from the receiver chamber. The same volume of fresh saline was added back to the receiver chamber after each aliquot removal to maintain a constant volume. The Ag and Ag/AgCl electrodes were also replaced by

fresh electrodes at predetermined times during the experiments. The duration of the experiments was approximately 1.5 h, which was at least six times longer than the transport lag time, 7 ± 5 min (average ± S.D.). The flux (J) and apparent permeability coefficient (P) were calculated at steady state under sink conditions (receiver concentrations ≤10% of the donor concentrations):

$$J = \frac{1}{A_D}\frac{\Delta Q}{\Delta t} \quad (1)$$

and

$$P = \frac{J}{C_D} \quad (2)$$

where C_D is the concentration of the permeant in the donor chamber, A_D the diffusional surface area, and $\Delta Q/\Delta t$ is the slope of the cumulative amount of the permeant transported across the membrane into the receiver chamber versus time plot. The donor and receiver samples were analyzed by a colorimetric method (Li et al., 2004b).

To evaluate the effects of permeant concentration upon transscleral iontophoretic transport, iontophoresis experiments were performed with Mn^{2+} and $MnEDTA^{2-}$ as the model permeants and the sclera. Passive experiments under the same conditions were the baseline control. The donor solutions in these experiments were 0.4, 4.0, and 40 mM Mn^{2+} in saline, 2 and 20 mM $MnEDTA^{2-}$ in saline, and 0.1 M $MnEDTA^{2-}$ in deionized water. These concentrations were similar to those used in the in vivo MRI studies for comparison with the MRI data in the studies.

2.3. In vivo MRI experiments

Animal MRI experiments were carried out with a GE SIGNA 1.5 T (NV/CVi gradient) clinical MRI system (GE Medical System Inc., Milwaukee, WI) with a temporal mandibular joint coil (TMJ coil: a double surface phased array coil set with 3 in. diameter) similar to those described previously (Li et al., 2004a). Dynamic MR imaging was performed, with T_1 (spin–lattice relaxation time) weighted spin-echo imaging technique. Unless otherwise specified, the imaging parameters were 400 ms TR, 9 ms TE, 256 readout matrix with 160 phase-encoding, and 2 signal averages to increase signal-to-noise ratio (SNR). Imaging field of view (FOV) was 12 cm in readout direction. Rectangular FOV with 50 or 75% reduction factor was used to reduce the imaging time in phase-encoding direction. The slice thickness was 2 mm with no spacing, resulting in spatial resolution of 0.47 mm × 0.47 mm × 2.0 mm (voxel). Each scan provided at least 10 image slices in transverse orientation to cover the whole eye, but only the images through the center of the eye and the iontophoresis application site would be presented in this paper. Prescanning was performed only once for the first data set at the beginning of the experiment, and the imaging parameters include the prescan results, such as transmitter and receiver gains. Imaging time for single time data was approximately 1 min. Data were usually acquired every 3 to 5 min during the experiments. All MRI experiments were carried out at least in duplicate.

After the rabbits were anesthetized with 25–50 mg/kg ketamine IM and 5–10 mg/kg xylazine IM, an electrode device with 0.4, 4.0, and 40 mM $MnCl_2$ in saline or 0.1 M $Na_2MnEDTA$ in water was placed on the conjunctiva/sclera in the superior cul-de-sac (under the upper eyelid) either near the limbus at the pars plicata/pars plana or far away from the limbus near the fornix for transscleral iontophoresis. The position of the electrode was maintained by fixing the wire of the electrode to the MRI coil with adhesive tape and by the pressure from the eyelid. An observation in the present study different from the previous study (Li et al., 2004a) was that the electrodes did not exert pressure on the eye. This is due to the different methods used to hold the electrode in the cul-de-sac and the restraint imposed with the animals in the present and previous studies. During iontophoresis, the position of the electrode was checked by comparing the relative electrode position to the anatomical structures of the eye in the MR images. Both the left and right eyes were used, but they were not used concurrently in the iontophoresis studies. The return electrode (approximately 4 cm^2 surface area) was placed on a piece of gauze pad (approximately 40 cm^2 surface area) wetted in saline and clamped to the ear on the opposite side of the treated eye. The wires to supply the direct current (dc), which ran between the dc current supply device and the electrodes, were twisted and the loop area was minimized to reduce possible noise contribution to MRI. Constant dc of 2 and 4 mA, approximately 10 and 20 mA/cm^2, was applied to the eye for 20 min. For $MnCl_2$, the donor electrode was the anode. For $Na_2MnEDTA$, the donor electrode was the cathode. 60-min iontophoresis experiments of Mn^{2+} were also conducted. In these experiments, after the initial 20-min iontophoresis of the permeant, the electrode device was replaced with fresh electrode devices that only contained saline (without the permeant) when iontophoresis was briefly paused at 20 and 40 min. These interruptions, which were less than one minute, were relatively short compared to the duration of the iontophoresis application. Fresh electrodes were required to sustain the long iontophoresis application because of the current dose capacity of the Ag electrode and the limited quantity of ions in the electrode chamber for conducting the electric current. For example, when the duration of the iontophoresis application exceeded the current dose capacity of the electrode, the resistance of the system would increase. The electrode would then need to be replaced to continue the iontophoresis application. The delivery and distribution of the probe ions in the eye were monitored by MRI during and after iontophoresis.

The iontophoresis condition of 20 min and 2 mA was selected in the present study because it was within the tolerable limit according to a previous human study (Parkinson et al., 2003). The higher current (4 mA) and longer duration (60 min) conditions were primarily selected for comparison. Whether these higher currents and longer duration conditions would be acceptable to human was beyond the scope of the present study and would remain to be examined in future studies. There was no apparent significant damage to the eye caused by iontophoresis and the device by visual observation, consistent with the current density levels (e.g., 25 mA/cm^2) suggested to be safe previously (Behar-Cohen et al., 2002; Hughes and Maurice, 1984).

2.4. MRI data interpretation

In manganese-enhanced MRI, Mn^{2+} ion and $MnEDTA^{2-}$ complex (the model permeants) enhance the relaxivity of the water protons, reduce the proton spin–lattice relaxation times, and enhance the signal in the MR images. The calibration curves of manganese-enhanced signal intensity versus Mn^{2+} and $MnEDTA^{2-}$ concentration were presented in previous studies (Li et al., 2004a,b). According to the data in these studies, the relationships between signal intensity and permeant concentration are parabolic. The very bright voxels (high signal intensities) in aqueous medium and vitreous humor in the MR images represent approximately 0.8 mM Mn^{2+} or 4 mM $MnEDTA^{2-}$. Above and below these concentration levels, the signal intensities gradually declined (darker voxels). Below approximately 0.02 mM Mn^{2+} and 0.1 mM $MnEDTA^{2-}$, there was essentially no signal enhancement. Due to the parabolic behavior, a range of different permeant concentration (e.g., 0.4, 4.0, and 40 mM $MnCl_2$) was used in the present study for MRI data interpretation. In addition, the concentration of the permeants in the tissues and other segments of the eye cannot be evaluated with the present technique because of possible interferences from Mn-tissue binding and the tissue proton relaxation times (Berkowitz et al., 2006; Watanabe et al., 2001). The MR images were analyzed with Scion Image program (Scion Corp., Frederick, MD). Tissues (fat tissues at the back outside the eye) away from the regions of interest were selected and their signals were used as references in the MR images. MR images with tissue reference signals outside the one-standard deviation range of the reference average were not used in the analysis. The distances between two points or two regions of interest were determined by the number of pixels (one pixel $\simeq$ 0.47 mm) between the two points in the images.

3. Results

3.1. In vitro results

Table 1 presents the fluxes and the apparent permeability coefficients of sclera for $MnCl_2$ at 0.4, 4 and 40 mM and $MnEDTA^{2-}$ at 2 mM, 20 mM and 0.1 M during 2-mA transscleral iontophoresis in vitro. The fluxes and permeability coefficients (i.e., the fluxes normalized by the donor concentrations) were calculated by Eq. (1). Passive transscleral permeation of Mn^{2+} and $MnEDTA^{2-}$ was determined in a previous study, and the permeability coefficients were 3.5×10^{-5} and 2.5×10^{-5} cm/s, respectively (Li et al., 2004b). These passive permeability coefficients are significantly lower than those of iontophoresis in the present study. From the table, the iontophoretic fluxes of the permeants increase with their donor concentrations when background electrolyte is present. The permeability coefficients of Mn^{2+} are significantly larger than those of $MnEDTA^{2-}$. This is due to the higher electromobility (or diffusion coefficient) of Mn^{2+} than that of $MnEDTA^{2-}$ and electroosmosis. At high donor concentrations such as 40 mM Mn^{2+} and 0.1 M $MnEDTA^{2-}$, the permeability coefficients were significantly lower than those at lower concentrations. The results in previous passive permeation studies in vitro suggested minimal interference from the counterions and little effects due to the different ionic strength in the donor and receiver upon transport across the sclera (Li et al., 2004b). However, during transscleral iontophoresis, the present results suggest counterion influence upon transport under an electric field. It is believed that when high concentration of the permeants was used, the higher ion concentration in the donor chamber than that in the receiver can lead to the situation that permeant fluxes become no longer proportional to the concentration of the permeants in the donor (Li et al., 2005), and lower normalized fluxes (the apparent permeability coefficients) would be observed.

3.2. Transscleral iontophoresis

Fig. 1 shows the MR images obtained after 20 min 2 mA iontophoresis with 4 and 40 mM Mn^{2+} and 0.1 M $MnEDTA^{2-}$ as the model permeants when the electrodes were placed on the conjunctiva/sclera near the limbus at the pars plana in vivo. At 0.4 mM Mn^{2+}, no significant MR signal was observed in the anterior and posterior chambers and the vitreous (data not shown), suggesting that ion penetration under these conditions was below the detection limit. At Mn^{2+} concentration of 4 mM, there is small signal enhancement in the anterior chamber in the eye (Fig. 1b). At 40 mM Mn^{2+} and 0.1 M $MnEDTA^{2-}$, the MR images show that Mn^{2+} and $MnEDTA^{2-}$ were primarily delivered into the anterior segment of the eye (Fig. 1a and c). In the MR images of 40 mM Mn^{2+}, the permeant was observed to travel as far as 1.5 mm into the posterior chamber and vitreous directly under the electrode/conjunctiva interface and remained there at least 1 h after iontophoresis (Fig. 1c). As expected from the in vitro data and the diffusion coefficients of the permeants, the

Table 1
Results of 2 mA transscleral iontophoresis in vitro

Permeant	Molecular weight	Diffusion coefficient ($\times 10^{-5}$ cm^2/s)[a]	Donor concentration (mM)	Flux (nmol/(cm^2 s))[b]	Permeability coefficient ($\times 10^{-5}$ cm/s)
Mn^{2+}	55	1.3	0.4	0.10 ± 0.02	26
Mn^{2+}	55	1.3	4	0.84 ± 0.32	21
Mn^{2+}	55	1.3	40	5.6 ± 1.2	14
$MnEDTA^{2-}$	343	0.9	2	0.18 ± 0.03	8.8
$MnEDTA^{2-}$	343	0.9	20	1.4 ± 0.1	7.0
$MnEDTA^{2-}$	343	0.9	100	6.0 ± 0.8	6.0

[a] From Li et al. (2004b).
[b] Mean ± S.D. (n = 3).

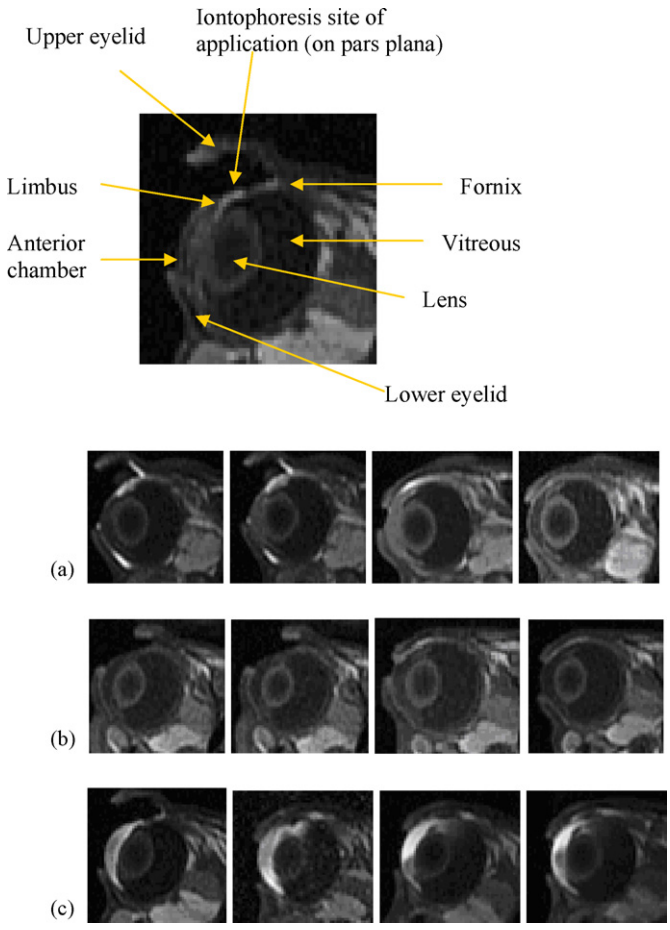

Fig. 1. Representative MR images of transscleral iontophoresis experiment in vivo of 2 mA of (a) 0.1 M $MnEDTA^{2-}$, (b) 4 mM Mn^{2+}, and (c) 40 mM Mn^{2+}. From left to right, images obtained at (a) 9 and 19 min during iontophoresis and 10 and 150 min after iontophoresis, (b) 9 and 20 min during iontophoresis and 50 and 100 min after iontophoresis, and (c) 20 min during iontophoresis and 10, 45, and 75 min after iontophoresis, respectively. The enlarged MR image shows the eyelids, anterior chamber, lens, vitreous, and the site of iontophoresis application. The electrode device appears as a low-signal dark rectangular object in the superior cul-de-sac. Enlarged image: obtained at 10 min during 2 mA 40 mM Mn^{2+} iontophoresis.

permeation of $MnEDTA^{2-}$ is slower than that of Mn^{2+} in vivo; $MnEDTA^{2-}$ does not travel as far back into the eye as Mn^{2+}. It was also noted that tear secretion increased during cathodal $MnEDTA^{2-}$ iontophoresis relative to that during anodal Mn^{2+} iontophoresis. A small pocket of tear with $MnEDTA^{2-}$ giving bright MR signals was observed in the inferior cul-de-sac. The signals from the tear were confirmed by removing the tear from the eye surface (and eliminating the signals) with tissue paper. The secretion can be related to the polarity of the electric current

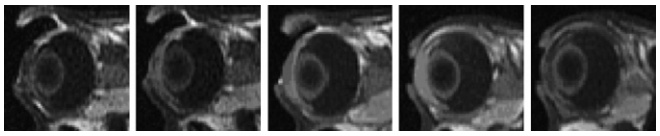

Fig. 3. Representative MR images of transscleral iontophoresis in vivo of 0.1 M $MnEDTA^{2-}$ and 4 mA when the electrode was placed on the sclera near the limbus. From left to right, images taken at 9 and 19 min during iontophoresis and 10, 40, and 150 min after iontophoresis.

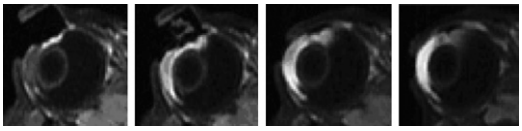

Fig. 4. Representative MR images of transscleral iontophoresis in vivo of 40 mM Mn^{2+} and 4 mA when the electrode was placed on the sclera near the limbus. From left to right, images obtained at 9 and 19 min during iontophoresis and 10 and 40 min after iontophoresis.

or the presence of high concentration EDTA or both. Consequently, the tears may prevent effective drug delivery if the donor chamber of the electrode device is not sealed from the tears on the eye. When the electrodes were placed on the sclera further away from the limbus towards the fornix, little ion penetration into the anterior chamber was observed (Fig. 2) and the permeant could not be delivered beyond the tissue barrier composed of the conjunctiva, superior rectus muscle, and sclera into the vitreous under the electrode. Permeant delivery into the vitreous or to the back of the eye was not observed after iontophoresis nor with iontophoresis of longer duration up to 60 min (data not shown) when the electrode was placed near the fornix.

Fig. 3 shows the MR images of 20 min 4-mA iontophoresis application with 0.1 M $MnEDTA^{2-}$ when the electrodes were placed on the conjunctiva/sclera next to the limbus in vivo. Fig. 4 shows the images of 40 mM Mn^{2+} under the same conditions. Although the 4 mA protocol seems to push the Mn^{2+} ions slightly further into the vitreous from the anterior segment of the eye compared to 2 mA, this difference is small. There is no significant enhancement in permeant penetration in the MR images as anticipated from doubling the current from 2 to 4 mA during iontophoresis.

The MR images during 60-min 2-mA in vivo iontophoresis application of 40 mM Mn^{2+} with the electrode placed on the conjunctiva/sclera next to the limbus are shown in Fig. 5. As can be seen in the figure, permeant penetration into the ciliary body, the anterior chamber, and the posterior chamber near the electrode occurred between 10 and 20 min. Further penetration towards the back of the eye can be observed at 40 min. At 60 min, permeant was observed in the vitreous near the site of electrode

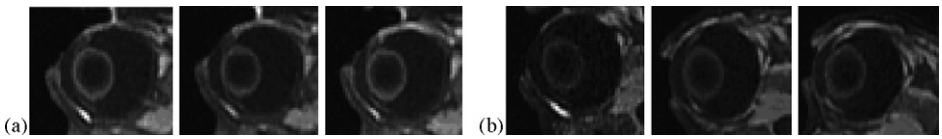

Fig. 2. Representative MR images of in vivo transscleral iontophoresis of (a) 0.1 M $MnEDTA^{2-}$ and (b) 40 mM Mn^{2+} at 2 mA with the electrode placed on the sclera away from the limbus and near the fornix. From left to right, images obtained at (a) 7 and 20 min during iontophoresis and 12 min after iontophoresis and (b) 19 min during iontophoresis and 7 and 57 min after iontophoresis.

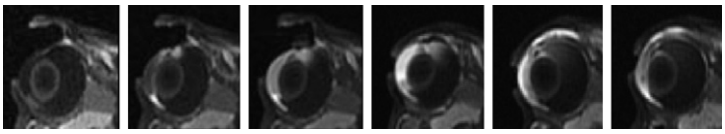

Fig. 5. Representative MR images obtained during and immediately after transscleral iontophoresis of 40 mM Mn^{2+} and 2 mA in vivo when the electrodes were placed on the sclera near the limbus. From left to right, at 10, 20, and 40 min during 60-min transscleral iontophoresis and 0, 1.5, and 3 h after iontophoresis.

placement. The distribution of the permeant from 20 to 60 min suggests that the route of permeant transport was from the ciliary body to the superior posterior chamber and the vitreous under the electrode. The MR images also suggest direct iontophoretically enhanced transport of the permeant from the ciliary body to the anterior chamber. However, the possibility that the permeant in the iris and the anterior chamber was carried from the choroid and ciliary body via local blood circulation (Wu et al., 1992) cannot be ruled out.

4. Discussion

4.1. Transscleral iontophoresis

Although only contrast agents were employed in the present study, they provide insights into the mechanisms of ocular delivery of drug ions of similar molecular size, charge, and/or electromobility. The delivery of drug ions is mainly related to these physicochemical parameters and should follow general physical and electrochemical principles when no specific interactions such as facilitated transport are involved. The results of the in vitro studies in Table 1 support this rationale. Table 2 presents the general trend of Mn^{2+} and $MnEDTA^{2-}$ delivery in the present and previous in vivo studies. Transscleral iontophoresis was shown to enhance the penetration of the permeant into the anterior chamber and into the posterior chamber near the ciliary body directly under the electrode/conjunctiva interface. In contrast to iontophoresis, subconjunctival injections (Li et al., 2004b) and passive diffusion (Li et al., 2004a) did not deliver a significant amount of the probe ions into the eye in vivo. The effects of the electric field upon drug delivery into the eye over passive diffusion are clearly demonstrated. It is of interest to note the similarity of permeant distribution in the eye after transscleral iontophoresis at the pars plana in vivo and after subconjunctival injection postmortem. In a previous subconjunctival injection postmortem study, permeants were mainly delivered into the anterior part of the eye by diffusion via the least resistive pathway in the ciliary body region (Li et al., 2004b). Ocular clearance plays an important role in hindering transscleral delivery of polar compounds into the eye (Lee and Robinson, 2004; Robinson et al., 2006). Particularly, blood vasculature clearance is a major barrier in transscleral transport (Li et al., 2004b). Conjunctival lymphatic clearance and other factors (Kim et al., 2004) also contribute to the transscleral barrier. The similarity of the results of transscleral iontophoresis in vivo and subconjunctival injection postmortem suggests that the applied electric field can potentially drive the permeants across the barrier due to clearance such as the blood vasculature barrier to enhance drug delivery.

Despite the enhancement effect of iontophoresis, the present and previous in vivo studies indicate that short iontophoresis applications (e.g., 20 min) of moderate electric current cannot directly deliver the ionic permeants to the tissue at the back of the eye away from the site of iontophoresis application; there was no indication of the permeants at the back such as near the optic nerve (below the detection limit) nor any sign of a penetration route via the vitreous to this location in the MR images in vivo. This is consistent with the electric fields, ion electromobilities, and electrotransport theory (Li et al., 2004a). Previous studies have shown drug delivery to the posterior segment of the eye with short iontophoresis applications of low to moderate current (Behar-Cohen et al., 2002; Voigt et al., 2002a, 2002b; Kralinger et al., 2003). Drugs were usually in small quantities in the choroid and retina in these studies. It was also found that drug concentration in the retina could increase after iontophoresis (Voigt et al., 2002b). It is speculated that the mechanism of posterior eye delivery to the tissues of more than a centimeter away from the iontophoresis application site under those circum-

Table 2
Assessment of permeants delivered into the eye based on the 40 mM Mn^{2+} and 0.1 M $MnEDTA^{2-}$ MRI studies in vivo[a]

Experiment	Anterior chamber	Ciliary body/posterior chamber near site of application	Vitreous near site of application
Passive delivery[b]	–	–	–
Subconjunctival injection[c]	–	–	–
20-min transscleral iontophoresis near the fornix at 2 mA	–	–	–[d]
20-min transscleral iontophoresis at the pars plana at 2 mA	xxx	xx	x
60-min transscleral iontophoresis at the pars plana at 2 mA	xxx	xxx	xxx
20-min transscleral iontophoresis at the pars plana at 4 mA	xxx	xx	x

[a] –, undetectable: below 0.02 mM; x, trace amount: 0.02–0.08 mM; xx, small amount: 0.08–0.3 mM; xxx, substantial amount: 0.3–2 mM; in the ROIs for Mn^{2+} and $MnEDTA^{2-}$.
[b] From Li et al. (2004a).
[c] From Li et al. (2004b).
[d] Subjected to the location of the ROI and the interpretation of the data.

stances may be due to local blood circulation. If this mechanism is true, Mn^{2+} and $MnEDTA^{2-}$ in these tissues at the back of the eye, if any, are likely to be below the MRI detection limit and cannot be located in the MR images of the present study.

4.2. Factors affecting transscleral iontophoresis

Iontophoresis generally enhances drug delivery by three mechanisms: electrophoresis, electroosmosis, and electroporation (Li et al., 2005; Eljarrat-Binstock and Domb, 2006). Electrophoresis is the facilitation of the movement of ionic species by the applied electric field. Electroosmosis assists (or retards) the transport of both neutral and charged species by electric field-induced convective solvent flow. Electroporation describes barrier alteration that increases the intrinsic permeability of the membrane. According to a previous in vitro study (Li et al., 2005), the effects of electroosmosis upon transscleral iontophoretic transport of small ionic permeants are secondary. The results in a recent MRI study suggest that electroporation of a transscleral tissue barrier, possibly of the retinal epithelial membrane, is a flux enhancing mechanism of transscleral iontophoresis (unpublished data).

According to electrotransport theory (Li et al., 2004a), the extent and penetration depth of iontophoretic delivery was expected to be related to the electric field and the duration of the iontophoresis application. The position of electrode placement was also expected to affect ocular iontophoretic delivery due to the anatomy of the eye—different transscleral routes of penetration and barriers (Cunha-Vaz, 1979; Worakul and Robinson, 1997; Robinson et al., 2006). When the applied electric current is increased, the electric field across the eye from the donor to the return electrodes increases, and iontophoretic delivery is expected to be enhanced. Results from previous transscleral iontophoresis studies are generally consistent with this trend. For example, iontophoresis studies of dexamethasone phosphate, methylprednisolone, amikacin, cefazolin, ticarcillin, and gentamicin showed an increase in delivery into the eye when the electric current of iontophoresis was increased (Barza et al., 1986; Behar-Cohen et al., 2002; Vollmer et al., 2002; Eljarrat-Binstock et al., 2005). In a study of the effects of current density upon iontophoretic delivery of fluorescein into the posterior segment of the eye, electric current density was shown to significantly affect transscleral delivery when the current density was above 40 mA/cm^2 (Maurice, 1986). In addition to the enhancement in delivery, deeper permeant penetration into the eye is also expected at higher electric current. However, it is difficult to determine the depth of penetration of a permeant in the eye in conventional pharmacokinetic studies.

In the present study, the effects of electric current levels were examined by comparing the in vivo results in transscleral iontophoresis at 2 and 4 mA when the electrode was placed on the pars plana near the limbus. Although both electric current levels show permeant transport into the anterior chamber and in the vicinity under the electrodes, the effects of electric current upon the amount of permeant delivered into the eye were not significant and difficult to be distinguished in the 2 and 4 mA MR images. A possible explanation to this is the limited amount of probe permeants provided in the electrode device. In a previous study, it took less than 20 min at 2 mA for Mn^{2+} to be completely unloaded from a similar electrode device (Li et al., 2004a). By increasing the electric current to 4 mA, the entire content of the permeant in the electrode would be depleted before the completion of the 20-min application for Mn^{2+}. The higher current would therefore mainly enhance the depth of penetration of the permeant into the eye rather than the amount delivered. It is possible that higher electric current density (higher electric field) may be more effective in delivering permeants across the clearance barrier or altering the transscleral barrier to enhance penetration into the eye. However, current densities higher than those employed in the present study (e.g., greater than 40 mA/cm^2) may be required for these effects to occur as suggested by the data in a previous study (Maurice, 1986). There is no significant enhancement of the amount of permeant delivered into the eye in the present 2 and 4 mA studies. The 4 mA MR results in the present study also do not show a significant enhancement in the depth of permeant penetration at the higher electric current. A possible explanation would be greater diversification of the electric field to other tissues when the higher electric current was applied across the eye.

Similar to the effects of electric current, the duration of the iontophoresis application can affect the extent of permeant delivery and the depth of permeant penetration into the eye. Previous iontophoresis studies showed an increase in delivery with longer iontophoresis application (Barza et al., 1986; Behar-Cohen et al., 2002; Vollmer et al., 2002b). The penetration depth effect was not studied because such effect is difficult to be examined with conventional pharmacokinetic methods. In the present study, because the electrode was replaced with blank saline electrodes after 20 min of iontophoresis application, extending the duration of the iontophoresis application from 20 to 60 min should only provide deeper penetration of the permeant into the eye, which is consistent with the MRI results.

The effects of electrode placement upon transscleral iontophoretic delivery were also investigated. It was expected that placing the electrode at the back of the eye in the superior culde-sac towards the fornix would enhance permeant delivery to the posterior segment of the eye. However, the MR images in the experiments of this electrode placement show that transscleral iontophoresis cannot deliver the permeants more than 1.5 mm from the electrode/conjunctiva interface into the eye when the electrode was placed at this position. This is consistent with the results in a previous in vivo study (Li et al., 2004a). According to the present MR images, it is not clear whether significant amounts of the permeants have penetrated through the sclera into the vitreous. If the total thickness of the conjunctiva, sclera, choroid, and retina is less than 0.5 mm, the MR results in the previous and present studies can be interpreted as the permeants getting across these barriers into the vitreous. However, the total barrier thickness under the electrode is greater than 0.9 mm due to the presence of the superior rectus muscle at the site of iontophoresis application; the superior muscle extends and thickens from the limbus to the fornix (from around 0.2 mm at the limbus to 0.4 mm at the site of iontophoresis application, unpublished data). Together with the effect of partial volume averaging, even

when the MR signals of the voxels at ∼1.0 to 1.5 mm from the device–conjunctiva interface are enhanced in the MR images, the permeants may not be in the vitreous. There was no evidence that the permeants were delivered into the vitreous when the electrode was placed near the fornix in the previous and present studies. For transscleral iontophoresis of electrode placement on the pars plana, significant amounts of the permeants were delivered to the ciliary body and the anterior chamber. Some permeant delivery was also observed in the posterior chamber near the electrode. To achieve permeant penetration further into the posterior segment of the eye, longer iontophoresis applications are required. The 60-min iontophoresis protocol showed a significant increase in the extent of permeant delivery into the posterior chamber compared with that of 20 min. Some permeant transport into the vitreous was observed after 40 min of iontophoresis application in these longer duration iontophoresis experiments.

5. Conclusion

The present study demonstrates that transscleral iontophoresis is more effective than subconjunctival injection and passive diffusion in ocular delivery of ionic permeants. Factors such as electrode placement, applied electric current, and duration of iontophoresis application were investigated. Ocular iontophoretic delivery was affected by the position of electrode placement and the duration of the application, but to a lesser extent by the electric current levels under the conditions studied. Iontophoresis enhances the transport of ionic permeants across the least resistive transscleral pathway (the ciliary body), and primarily delivers the permeants to the anterior segment of the eye when the electrodes are placed on the conjunctiva/sclera near the limbus. When the electrode was placed near the fornix, no penetration of the permeants into the vitreous was detected during and after iontophoresis. Direct delivery of the permeants deep into the vitreous and to the retina at the back of the eye was not observed with the duration and electric current used in the present iontophoresis study. Caution must also be taken in designing an ocular iontophoresis device and in analyzing the iontophoresis data because the total amount of permeant provided in the iontophoresis device can be a factor. These findings continue to support the utility of MRI as a noninvasive technique in ocular drug delivery research and testing.

Acknowledgements

This research was supported in part by NIH Grant EY 015181. The authors thank Dr. Rajan P. Kochambilli for his help in the preparation of some experiments, and Dr. Paul S. Bernstein for helpful discussion.

References

Barza, M., Peckman, C., Baum, J., 1986. Transscleral iontophoresis of cefazolin, ticarcillin, and gentamicin in the rabbit. Ophthalmology 93, 133–139.

Behar-Cohen, F.F., Parel, J.M., Pouliquen, Y., Thillaye-Goldenberg, B., Goureau, O., Heydolph, S., Courtois, Y., De Kozak, Y., 1997. Iontophoresis of dexamethasone in the treatment of endotoxin-induced-uveitis in rats. Exp. Eye Res. 65, 533–545.

Behar-Cohen, F.F., El Aouni, A., Gautier, S., David, G., Davis, J., Chapon, P., Parel, J.M., 2002. Transscleral coulomb-controlled iontophoresis of methylprednisolone into the rabbit eye: influence of duration of treatment, current intensity and drug concentration on ocular tissue and fluid levels. Exp. Eye Res. 74, 51–59.

Berkowitz, B.A., Roberts, R., Goebel, D.J., Luan, H., 2006. Noninvasive and simultaneous imaging of layer-specific retinal functional adaptation by manganese-enhanced MRI. Invest Ophthalmol. Vis. Sci. 47, 2668–2674.

Cunha-Vaz, J., 1979. The blood-ocular barriers. Surv. Ophthalmol. 23, 279–296.

Eljarrat-Binstock, E., Raiskup, F., Frucht-Pery, J., Domb, A.J., 2005. Transcorneal and transscleral iontophoresis of dexamethasone phosphate using drug loaded hydrogel. J. Contr. Rel. 106, 386–390.

Eljarrat-Binstock, E., Domb, A.J., 2006. Iontophoresis: a non-invasive ocular drug delivery. J. Contr. Rel. 110, 479–489.

Hughes, L., Maurice, D.M., 1984. A fresh look at iontophoresis. Arch. Ophthalmol. 102, 1825–1829.

Kim, H., Robinson, M.R., Lizak, M.J., Tansey, G., Lutz, R.J., Yuan, P., Wang, N.S., Csaky, K.G., 2004. Controlled drug release from an ocular implant: an evaluation using dynamic three-dimensional magnetic resonance imaging. Invest Ophthalmol. Vis. Sci. 45, 2722–2731.

Kralinger, M.T., Voigt, M., Kieselbach, G.F., Hamasaki, D., Hayden, B.C., Parel, J.M., 2003. Ocular delivery of acetylsalicylic acid by repetitive coulomb-controlled iontophoresis. Ophthalmic. Res. 35, 102–110.

Lam, T.T., Edward, D.P., Zhu, X.A., Tso, M.O., 1989. Transscleral iontophoresis of dexamethasone. Arch. Ophthalmol. 107, 1368–1371.

Lee, T.W., Robinson, J.R., 2004. Drug delivery to the posterior segment of the eye II: development and validation of a simple pharmacokinetic model for subconjunctival injection. J. Ocul. Pharmacol. Ther. 20, 43–53.

Li, S.K., Jeong, E.K., Hastings, M.S., 2004a. Magnetic resonance imaging study of current and ion delivery into the eye during transscleral and transcorneal iontophoresis. Invest Ophthalmol. Vis. Sci. 45, 1224–1231.

Li, S.K., Molokhia, S.A., Jeong, E.K., 2004b. Assessment of subconjunctival delivery with model ionic permeants and magnetic resonance imaging. Pharm. Res. 21, 2175–2184.

Li, S.K., Zhang, Y., Zhu, H., Higuchi, W.I., White, H.S., 2005. Influence of asymmetric donor–receiver ion concentration upon transscleral iontophoretic transport. J. Pharm. Sci. 94, 847–860.

Maurice, D.M., 1986. Iontophoresis of fluorescein into the posterior segment of the rabbit eye. Ophthalmology 93, 128–132.

Parkinson, T.M., Ferguson, E., Febbraro, S., Bakhtyari, A., King, M., Mundasad, M., 2003. Tolerance of ocular iontophoresis in healthy volunteers. J. Ocul. Pharmacol. Ther. 19, 145–151.

Robinson, M.R., Lee, S.S., Kim, H., Kim, S., Lutz, R.J., Galban, C., Bungay, P.M., Yuan, P., Wang, N.S., Kim, J., Csaky, K.G., 2006. A rabbit model for assessing the ocular barriers to the transscleral delivery of triamcinolone acetonide. Exp. Eye Res. 82, 479–487.

Voigt, M., Kralinger, M., Kieselbach, G., Chapon, P., Anagnoste, S., Hayden, B., Parel, J.M., 2002a. Ocular aspirin distribution: a comparison of intravenous, topical, and coulomb-controlled iontophoresis administration. Invest Ophthalmol. Vis. Sci. 43, 3299–3306.

Voigt, M., de Kozak, Y., Halhal, M., Courtois, Y., Behar-Cohen, F., 2002b. Down-regulation of NOSII gene expression by iontophoresis of anti-sense oligonucleotide in endotoxin-induced uveitis. Biochem. Biophys. Res. Commun. 295, 336–341.

Vollmer, D.L., Szlek, M.A., Kolb, K., Lloyd, L.B., Parkinson, T.M., 2002. In vivo transscleral iontophoresis of amikacin to rabbit eyes. J. Ocul. Pharmacol. Ther. 18, 549–558.

Watanabe, T., Michaelis, T., Frahm, J., 2001. Mapping of retinal projections in the living rat using high-resolution 3D gradient-echo MRI with Mn^{2+}-induced contrast. Magn. Reson. Med. 46, 424–429.

Worakul, N., Robinson, J.R., 1997. Ocular pharmacokinetics/pharmacodynamics. Eur. J. Pharm. Biopharm. 44, 71–83.

Wu, J.C., Jesmanowicz, A., Hyde, J.S., 1992. Anterior segment high resolution MRI: aqueous humor dynamics observed using contrast agents. Exp. Eye Res. 54, 145–148.

Yoo, S.H., Dursun, D., Dubovy, S., Miller, D., Alfonso, E., Forster, R.K., Behar-Cohen, F.F., Parel, J.M., 2002. Iontophoresis for the treatment of paecilomyces keratitis. Cornea 21, 131–132.